Ritonavir induces endoplasmic reticulum stress and sensitizes sarcoma cells toward bortezomib-induced apoptosis

Marianne Kraus,[1] Elke Malenke,[1] Jeannette Gogel,[1] Holger Müller,[1] Thomas Rückrich,[1] Herman Overkleeft,[2] Huib Ovaa,[3] Ewa Koscielniak,[4] Jörg Thomas Hartmann,[1] and Christoph Driessen[1,5]

[1]Department of Medicine II, University of Tübingen, Tübingen, Germany; [2]Department of Chemistry, Leiden University, Leiden, The Netherlands; [3]Division of Cellular Biochemistry, The Netherlands Cancer Institute, Amsterdam, The Netherlands; [4]Olgahospital, Stuttgart, Germany; and [5]Department of Oncology and Hematology, Cantonal Hospital, St. Gallen, St. Gallen, Switzerland

Abstract

The biosynthesis of immunoglobulin leads to constitutive endoplasmic reticulum (ER) stress in myeloma cells, which activates the unfolded protein response (UPR). The UPR promotes protein folding by chaperones and increases proteasomal degradation of misfolded protein. Excessive ER stress induces apoptosis and represents a molecular basis for the bortezomib sensitivity of myeloma. Most solid malignancies such as sarcoma, by contrast, are poorly bortezomib sensitive and display low levels of ER stress. We hypothesized that pharmacologic induction of ER stress might sensitize malignancies to bortezomib treatment. We show that the HIV protease inhibitor ritonavir induces ER stress in bortezomib-resistant sarcoma cells. Ritonavir triggered the UPR, decreased the degradation of newly synthesized protein, but did not directly inhibit proteasomal active sites in the therapeutic dose range in contrast to bortezomib. Whereas neither bortezomib nor ritonavir monotherapy translated into significant apoptosis at therapeutic drug levels, the combination strongly increased the level of ER stress and activated PERK, IRE1, and ATF6, synergistically induced CHOP, JNK, caspase-4, and caspase-9, and resulted in >90% apoptosis. In summary, ritonavir increases the level of ER stress induced by bortezomib, which sensitizes bortezomib-resistant cells to bortezomib-induced apoptosis. Ritonavir may therefore be tested clinically to improve the sensitivity of solid malignancies toward bortezomib treatment. [Mol Cancer Ther 2008;7(7):1940–8]

Introduction

The therapeutic effect of the proteasome inhibitor bortezomib has been disappointing in solid malignancies in contrast to the treatment of myeloma and selected B-cell neoplasmas (1). Therefore, the identification of combination partners to exploit the mechanism of action of bortezomib is warranted.

The 26S proteasome is responsible for the bulk of cellular protein destruction and is essential for eukaryotic life (2). Bortezomib treatment with the established 1.3 mg/m^2 schedule every 72 h results in peak plasma concentrations between 10 and 20 nmol/L followed by rapid clearance from the bloodstream, leading to intermittent inhibition of the rate-limiting β5-type active subunit and to a lesser extent of the β1 active sites (3–5). The proteasome is part of the endoplasmic reticulum (ER)–associated machinery for protein degradation (ERAD) that removes misfolded protein from the ER for cytosolic degradation. Proteasome inhibition thus results in the accumulation of misfolded proteins in the ER, which induces the unfolded protein response (UPR). The UPR involves three major regulatory mechanisms: (*a*) it decreases the rate of bulk translation, (*b*) it increases the synthesis of chaperones such as BiP or other heat shock proteins, and (*c*) it augments the efficiency of ERAD. The UPR is triggered via three major pathways: the PERK, ATF6, and IRE1 pathways. Excess activation of the UPR leads to a so-called terminal or overwhelming UPR, which directly induces apoptosis via mitochondria-dependent and mitochondria-independent pathways involving CHOP, JNK, and caspase-4 (6, 7).

Myeloma cells are characterized by a constitutively active UPR, which clearly distinguishes them from most other types of malignancies (6, 8). This represents the molecular basis for the exceptional sensitivity of myeloma toward bortezomib (9). Thus, to exploit the therapeutic potential of bortezomib in non-B-cell malignancies, prior pharmacologic induction of ER stress by appropriately targeted drugs may be required (10). The HIV protease inhibitor ritonavir interferes with the ERAD machinery and shows activity against lymphoid malignancies and sarcoma (11–15). We here show that ritonavir is a potent inducer of the UPR in sarcoma cells and renders sarcoma cells sensitive toward therapeutic doses of bortezomib.

Materials and Methods

Cell Lines

The cell lines HT1080 and RD-ES (human fibrosarcoma and Ewing's sarcoma; American Type Culture Collection)

Received 12/6/07; revised 5/6/08; accepted 5/7/08.

Grant support: Deutsche Forschungsgemeinschaft SFB 685 and Deutsche Krebshilfe (C. Driessen).

The costs of publication of this article were defrayed in part by the payment of page charges. This article must therefore be hereby marked *advertisement* in accordance with 18 U.S.C. Section 1734 solely to indicate this fact.

Note: J.T. Hartmann and C. Driessen share senior authorship.

Requests for reprints: Christoph Driessen, Department of Oncology and Hematology, Cantonal Hospital St. Gallen, Rorschacherstrasse, 9001 St. Gallen, Switzerland. Phone: 41-71-494-1162; Fax: 41-71-494-6317. E-mail: christoph.driessen@kssg.ch

doi:10.1158/1535-7163.MCT-07-2375

and RPMI8226 and AMO-1 (myeloma; U. Keilholz, Department of Hematology) were maintained in FCS-supplemented RPMI 1640 with penicillin/streptomycin. Cells were treated with bortezomib (Ortho Biotech), ritonavir (Abbott), 6 μg/mL tunicamycin, 100 nmol/L thapsigargin, or 50 μmol/L NLVS (16) for 16 h, if not stated otherwise.

Apoptosis and Cell Cycle Analysis

For fluorescence-activated cell sorting–based analysis of apoptosis and cell cycling, cells were suspended in binding buffer [10 mmol/L HEPES/NaOH (pH 7.4), 140 mmol/L NaCl, 2.5 mmol/L $CaCl_2$] to identify early and late apoptosis or in hypotonic lysis buffer [0.1% (w/v) sodium citrate, 0.1% (v/v) Triton X-100, and 50 μg/mL propidium iodide] to assess DNA content indicative of the different cell cycle phases. Apoptosis was detected with the Annexin V-PE Apoptosis Detection Kit I (BD PharMingen) according to the manufacturer's instructions. Cell cycle phases were investigated as described in ref. 17.

Proliferation Assay

The CellTiter 96 MTS assay (Promega) was used according to the manufacturer's instructions. Results represent mean of quadruplicate wells in one of at least three independent experiments.

Active Site Labeling

Affinity labeling of active proteasomes using the proteasome-specific affinity probe dansyl-Ahx_3L_3VS (DALVS) was done as described (18). Equal amounts of total cellular protein were resolved by SDS-PAGE and labeled species were visualized by Western blot using a rabbit polyclonal dansyl-sulfonamidohexanoyl-specific antibody (Molecular Probes). Labeling experiments were repeated at least twice in an independent fashion, and representative results are displayed.

Electrophoresis and Western blots

SDS-PAGE and Western blot was done on precast 12% gels as described before (19).

The anti-CHOP (Gadd153; Santa Cruz Biotechnology), anti-BiP (Grp78), anti-p38, anti-pT180/pY182-p38, anti-ERK1, anti-pT202/pY204-ERK1, anti-JNK/SAPK, anti-pT183/pY185-JNK/SAPK (all from Becton Dickinson), anti- HSP70 (Dianova), anti-IRE1α, anti-eIF2α, and anti-pS51eIF2α (Cell Signaling Technology), anti-caspase-4, anti-ATF6 antibodies (Biomol), thapsigargin and tunicamycin (Biomol) were obtained commercially. Antibodies against caspase-9 and caspase-8 were kindly provided by S. Wesselborg (University of Tübingen). The PARP-1 antibody detects the p85 spliced form (Promega). The anti-PDI rabbit antiserum was provided by H. Ploegh (Massachusetts Institute of Technology).

Metabolic Labeling

For metabolic labeling of protein biosynthesis (20), RD cells were treated with inhibitors for 16 h, adjusted for equal cell numbers, and starved 20 min in methionine/cysteine-free medium at 37°C. Cells were subsequently incubated with [^{35}S]methionine/cysteine cell labeling mix (GE Healthcare) for 15 min (pulse). After intensive washing, cells were lysed, adjusted for total protein, precipitated with ice-cold 10% TCA on filter paper, and washed with ethanol and acetone before incorporated radioactivity was measured in a scintillation counter.

To determine the relative rate of protein degradation, ^{35}S-labeled cells were washed to remove nonincorporated radioactivity and further incubated at 37°C in complete medium for 60 min (chase). The difference between the incorporated radioactivity after the pulse (arbitrarily set as 100%) and the chase served to assess the rate of bulk protein degradation.

Reverse Transcription and PCR

RNA was isolated from HT1080 cells (RNeasy Mini kit, Qiagen). Aliquots of 1 μg total RNA were reverse transcribed in the presence of oligo(dT) primer, random primer and AMV reverse transcriptase (Promega). cDNA products (15 μL) were used for a 24-cycle PCR in a thermal cycler (Perkin-Elmer 9700) using specific primers for XBP-1 (forward CCTTGTGGTTGAGAACCAGG and reverse TCTCTGTCTCAGAGGGGATC) provided by H. Jäck (University of Erlangen). PCR products were digested with *Pst*I (Invitrogen), separated on 1.5% agarose gels, and visualized with ethidium bromide. IRE1α endonuclease activity splices inactive XBP-1 into the 26-bp smaller active form, which is resistant to *Pst*I cleavage.

Results

Ablation of Proteasomal β1 and β5 Activity Induces Little Cytotoxicity in Sarcoma Cells

Human myeloma (AMO-1 and RPMI 8662) and sarcoma cell lines (RD, Ewing's sarcoma; HT1080, fibrosarcoma) were incubated with increasing concentrations of bortezomib and the cell viability assessed by MTS test (Fig. 1A). Although bortezomib induced robust cytotoxicity at therapeutic concentrations (10-20 nmol/L) in myeloma cells, these drug levels had little influence on the viability of the sarcoma cells.

The activity-based probe DALVS specifically and irreversibly binds to both the immunoproteasome and the constitutive proteasome active sites when intact cells are incubated with the probe and allows visualization of active proteasome species (18). All four bortezomib-treated cell lines were therefore incubated with DALVS followed by SDS-PAGE and anti dansyl blot (Fig. 1B). Two dominant polypeptide signals were visualized representing the active proteasomal species. The upper ~28-kDa signal comprised the proteasomal β2 and the β2i subunits, whereas the 20-kDa signal combined polypeptides from both the constitutive and the immunoproteasome β1 and β5 species, consistent with published data (18, 21). The relative intensity of these two signals differed between the individual cell types: although the 20-kDa signal was much weaker in relation to the 28-kDa signal in the bortezomib-sensitive myeloma cell lines, it appeared to be at least similar intensity in the sarcoma cells. This is in agreement with previous findings, showing that bortezomib-sensitive cells are characterized by a low relative activity of β1/β5 type of subunits (21). Bortezomib treatment in concentrations above 10 nmol/L essentially eliminated the β1/β5

types of activity signals in the myeloma cells and the RD sarcoma line. The dose response of the inhibition of the β1/β5 signals by bortezomib differed between the two types of sarcoma cells (elimination of the respective activity between 5 and 10 nmol/L in RD cells versus between 20 and 40 nmol/L in HT1080); however, this did not mirror differential bortezomib sensitivity. Similarly, the difference in bortezomib sensitivity between RD and myeloma cells could not be explained by variable degrees of proteasome inhibition alone. These data show that sarcoma cells can compensate intermittent complete ablation of proteasomal β1/β5 type of activity by bortezomib in contrast to myeloma cells.

Bortezomib treatment resulted in a concentration-dependent increase in the expression of BiP and PDI in sarcoma cells comparable with tunicamycin (Fig. 1C). This UPR induction was visible at bortezomib levels of 20 nmol/L, indicating that functional ablation of β1/β5 type of proteasome subunits by therapeutic levels of bortezomib results in UPR induction in sarcoma cells, which does not translate into significant apoptosis.

Ritonavir Induces the UPR in Sarcoma Cells without Inhibition of Proteasomal Active Sites

Because ritonavir modulates the UPR and proteasome function in human monocytes (11, 13), we addressed proteasome activity and UPR induction in sarcoma cells. Ritonavir induced CHOP, BIP, and HSP70 in HT1080 cells and similarly induced CHOP, BIP, and PDI in RD cells (Fig. 2A, *top* and *middle*). We failed to induce HSP70 expression by either ritonavir or tunicamycin in RD cells (data not shown), whereas tunicamycin, but not ritonavir, induced PDI in HT1080 cells. This suggests that the UPR of different tumor cell lines may differentially respond to given UPR stimuli such as ritonavir or tunicamycin by differential regulation of ER chaperones. By contrast, myeloma cells showed a constitutive expression of UPR proteins that was not further increased by either bortezomib (20 nmol/L), ritonavir (40 μmol/L), or tunicamycin (*bottom*). The maximum effect of ritonavir on the UPR in sarcoma cells was observed at concentrations that exceeded the therapeutic dose of the drug (20 μmol/L). Within the therapeutic range, only minimal UPR induction, as defined by up-regulation of either PDI or HSP70, was visible, if any. Activation of the terminal UPR, as suggested by up-regulation of CHOP, was only observed at ritonavir levels exceeding 20 μmol/L. Consistent with this, therapeutic concentrations of ritonavir did not induce cytotoxicity, whereas high doses of the drug were cytotoxic (Fig. 2B). To exclude a direct inhibitory effect of ritonavir on the proteasome active sites, we assessed the activity profile of proteasome subunits in ritonavir-treated sarcoma cell lines using DALVS. We observed no change in the activity of proteasomal β1, β2, and β5 types of subunits at ritonavir concentrations up to 40 μmol/L.

We next assessed changes in the major pathways of UPR induction as well as in the caspases involved in mediating ER stress-mediated apoptosis (Fig. 2D). Up-regulation of IRE1α was already observed at therapeutic levels of ritonavir, whereas only higher concentrations also induced increased levels of both full-length and cleaved ATF6 as well as p-eIF2α, indicating PERK activity. Although minimal cleavage of caspase-8 was observed in samples exposed to ritonavir, we did not observe a concentration-dependent increase. Also, active caspase-4 was not induced by ritonavir alone. Caspase-9 was activated at 80 μmol/L ritonavir but not at therapeutic levels. Thus, at therapeutic ritonavir levels, IRE1 is the major UPR-inducing pathway

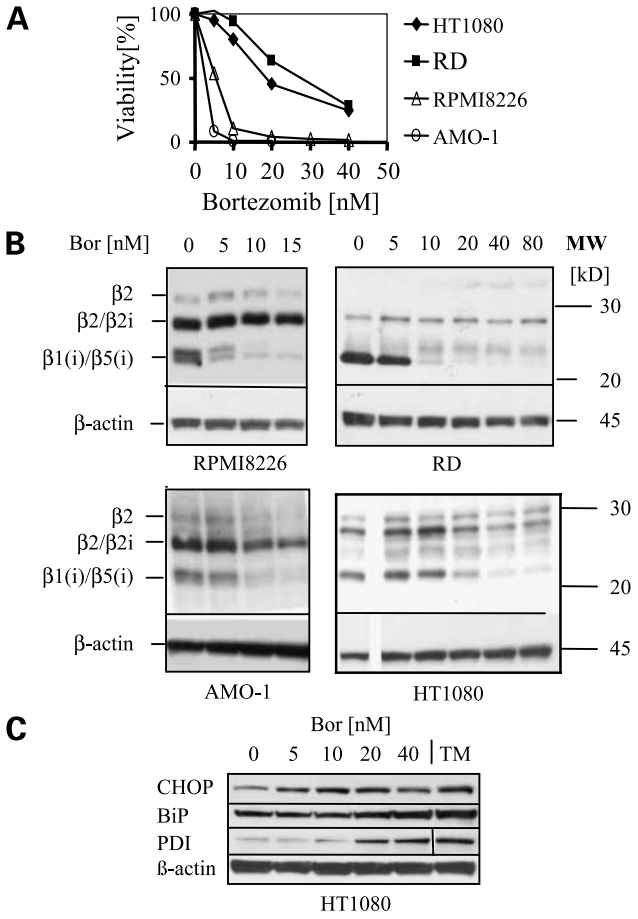

Figure 1. Ablation of proteasomal β5 and β1 activity induces ER stress but causes little cytotoxicity in sarcoma cells. **A,** sarcoma cell lines are insensitive to bortezomib. The sensitivity of the sarcoma cell lines RD and HT1080 and myeloma cell lines AMO-1 and RPMI8226 toward bortezomib was tested in a viability assay (MTS). Mean absorption values from quadruplicate samples are presented as percent relative to the untreated control. **B,** bortezomib effectively inhibits the enzymatic activity of β1 and β5 proteasomal subunits in both myeloma and sarcoma cells. The same types of cells were incubated with bortezomib at the concentrations indicated, followed by labeling of active proteasomal subunits in intact cells, using DALVS. Equal amounts of total protein were resolved by SDS-PAGE and active proteasomal polypeptides were visualized by Western blot against the dansyl moiety of the covalent proteasome label. **C,** bortezomib induces ER stress in sarcoma cells. The sarcoma cell line HT1080 was treated with up to 40 nmol/L bortezomib. After cell lysis, equal amounts of protein were resolved by SDS-PAGE and Western blots against the UPR-related proteins CHOP, BiP, and PDI were done. Cells treated with tunicamycin (*TM*; 6 μg/mL) served as a positive control and the Western blot against β-actin as loading control.

activated, whereas significant activation of caspases or direct inhibition of proteasomal active sites was not observed.

Ritonavir Sensitizes Sarcoma Cells toward Bortezomib-Induced UPR Activation and Apoptosis

The combination of both agents at therapeutic concentrations (20 nmol/L bortezomib and 20 μmol/L ritonavir; Fig. 3A, *top*) resulted in a markedly stronger UPR-induction (PDI, CHOP, BiP, and HSP70) compared with either drug alone. A very similar pattern was observed, when thapsigargin or tunicamycin were analyzed the same way. With any of these three UPR-inducing agents, the combination with bortezomib increased the expression of ER-resident chaperones, led to elevated CHOP levels, and induced cleaved PARP-1, suggesting a synergistic induction of apoptosis with bortezomib. Of note, this was not mediated by a direct synergistic effect of ritonavir and bortezomib on the activity pattern of the proteasome (Fig. 3B), which was not grossly influenced by 20 μmol/L ritonavir.

When assessed by MTS test (Fig. 3C), the combination of bortezomib and ritonavir at therapeutic concentrations (20 nmol/L and 20 μmol/L, respectively) resulted in >90% cell death. This effect was synergistic by nature, because the combination of bortezomib in subtoxic concentrations (~90% cell viability in RD cells with 20 nmol/L bortezomib and 80% viability in HT1080 cells treated with 10 nmol/L bortezomib) with concentrations of ritonavir that lacked a direct cytotoxic effect (100% viability of both cell types with 20 μmol/L ritonavir monotherapy) resulted in robust cytotoxicity (~90% cell death in RD and HT1080 cells, respectively). When thapsigargin or tunicamycin were used in combination with bortezomib, we similarly observed synergistic induction of cell death, although the effect observed was less strong and restricted to therapeutic peak levels of bortezomib.

We consecutively analyzed the upstream regulator and downstream effector pathways of the UPR by Western blot (Fig. 3D). Compared with untreated controls, all three

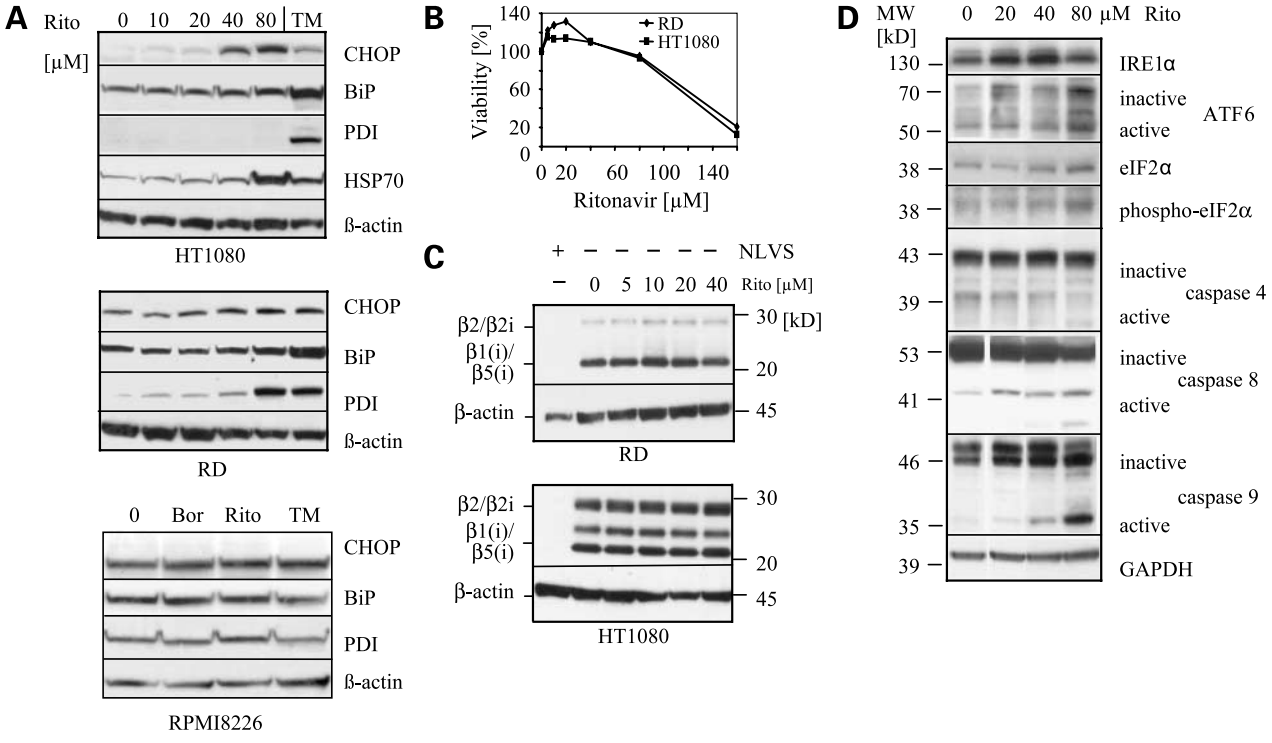

Figure 2. Ritonavir induces the UPR in sarcoma cells without direct inhibition of proteasomal subunit activity. **A,** ritonavir induces the UPR in sarcoma cell lines in contrast to myeloma. *Top* and *middle,* HT1080 and RD cells were incubated with increasing concentrations of ritonavir. Equal amounts of protein were resolved by SDS-PAGE and Western blots against the UPR-related proteins CHOP, BiP, HSP70, and PDI were done. Cells treated with tunicamycin (6 μg/mL) served as a positive control for ER stress induction. *Bottom,* RPMI 8226 myeloma cells were incubated with either ritonavir (40 μmol/L), bortezomib (20 nmol/L), or tunicamycin (6 μg/mL) as in Fig. 1 and in **A**, and the expression of the UPR-related proteins was similarly assessed by Western blot. **B,** therapeutic plasma levels of ritonavir are not cytotoxic for sarcoma cell lines. RD and HT1080 cells were subjected to ritonavir treatment at the concentrations indicated, and cell viability relative to the untreated control was assessed by MTS assay. **C,** activity of proteasomal subunits is not affected by therapeutic levels of ritonavir. Human sarcoma cell lines RD and HT1080 were incubated with ritonavir at concentrations up to 40 μmol/L, followed by labeling of active proteasomal subunits in intact cells, using DALVS. Cells were also incubated with the proteasome inhibitor NLVS before labeling to show the activity-based nature and specificity of DALVS labeling. Equal amounts of total protein were resolved by SDS-PAGE and active proteasomal polypeptides visualized by Western blot. **D,** ritonavir induces IRE1α at therapeutic drug levels, whereas caspase-9 is triggered at higher concentrations. Human HT1080 cells were incubated with ritonavir at concentrations up to 80 μmol/L for 24 h. Equal amounts of protein were resolved by SDS-PAGE and Western blots against key proteins for UPR induction and UPR-induced apoptosis (IRE1α, eIF2α, ATF6, caspase-4, caspase-8, and caspase-9) were done.

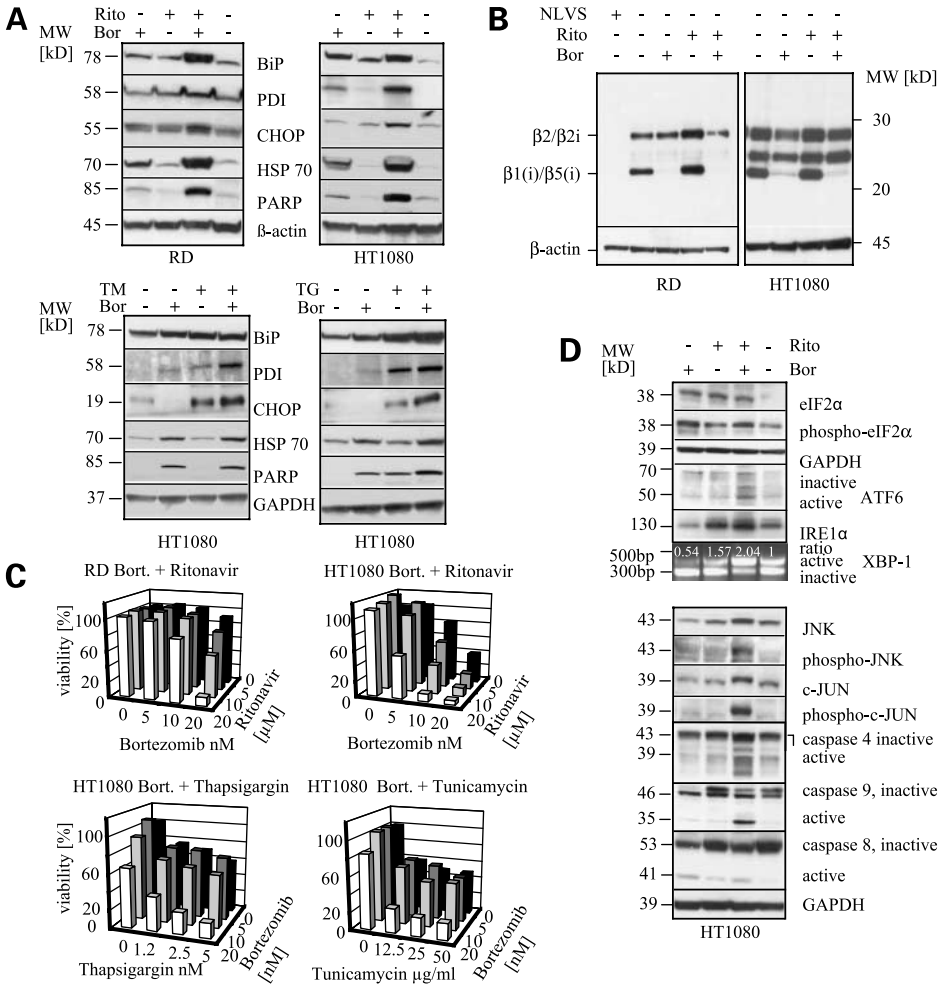

Figure 3. Ritonavir at therapeutic plasma levels amplifies the UPR induction by bortezomib, which is then sufficient to translate into apoptosis. **A,** RD and HT1080 sarcoma cells were treated either with 20 nmol/L bortezomib, 20 μmol/L ritonavir, or the combination of both. For direct comparison, HT1080 cells were treated either with 20 nmol/L bortezomib, 2.5 μg/mL tunicamycin, 12.5 nmol/L thapsigargin, or the combination. Equal amounts of protein were resolved by SDS-PAGE and Western blots against the UPR-related proteins BiP, PDI, CHOP, HSP70, and the apoptosis-related protein PARP (cleaved fragment is shown) were done. **B,** ritonavir treatment does not inhibit proteasomal subunits that remain active after bortezomib treatment. Human sarcoma cell lines RD and HT1080 were incubated with either ritonavir (20 μmol/L), bortezomib (20 nmol/L), or the combination of both, followed by labeling of active proteasomal subunits in intact cells, using DALVS, as detailed in Materials and Methods. DALVS selectively and irreversibly binds to β1/β2/β5 polypeptides of the proteasome in an activity-dependent manner and carries a dansyl moiety that allows specific detection. Cells incubated with the proteasome inhibitor NLVS (50 μmol/L) before labeling served as controls. Equal amounts of total protein were resolved by SDS-PAGE followed by Western blot against the dansyl moiety of the probe. **C,** combined treatment with therapeutic doses of ritonavir (20 μmol/L) and bortezomib (20 nmol/L) results in 7-fold reduction of cell viability compared with either monotherapy. RD and HT1080 cells were subjected to ritonavir and bortezomib at the concentrations indicated. To directly compare with established agents that induce the UPR, HT1080 cells were also subjected to either tunicamycin or thapsigargin in combination with bortezomib. Cell viability was measured by MTS assay. Representative of six experiments. Mean of quadruplicate samples. **D,** ritonavir and bortezomib differentially trigger UPR activation and synergistically activate JNK and caspase-4/caspase-9 apoptotic pathways. *Top,* human sarcoma cell line HT1080 was incubated with either ritonavir (20 μmol/L), bortezomib (20 nmol/L), or the combination of both. Equal amounts of protein were resolved by SDS-PAGE, and Western blots against key proteins of the major pathways that trigger the UPR were done (eIF2α, ATF6, and IRE1α). In addition, we determined the ratio of the spliced (mature) form of XBP-1 mRNA to its nonspliced version (*bottom*). To this end, XBP-1-specific reverse transcription-PCR was done and the amplificates were digested with *Pst*I, which selectively cleaves the unspliced version of XBP-1. Products were separated by 1.5% agarose gel and stained with ethidium bromide. The relative ratio (spliced/nonspliced) between the spliced, *Pst*I-resistant, mature version of XBP-1 and the *Pst*I-derived cleavage fragments derived from the nonspliced, immature XBP-1 was calculated based on quantitative analysis of the respective fluorescence signals using a fluorescence scanner. The relative ratio is indicated in each lane. *Bottom,* HT1080 cells were incubated with either ritonavir (20 μmol/L), bortezomib (20 nmol/L), or the combination of both as before. The phosphorylation of JNK and c-Jun as well as the activation of the caspase-4, caspase-8, and caspase-9 was assessed by Western blotting.

pathways (PERK, ATF6, and IRE1) were activated in cells treated with the drug combination. However, bortezomib and ritonavir affected the individual pathways in a differential fashion: although bortezomib increased the levels of p-eIF2α in sarcoma cells, it did not induce expression of IRE1. Ritonavir, by contrast, significantly induced IRE1 expression already at 20 μmol/L but did not affect the levels of p-eIF2α. This also translated into

different ratios between the spliced, mature XBP-1 and its nonspliced progenitor: whereas bortezomib treatment reduced the relative contribution of mature XBP-1 by close to 50%, ritonavir increased mature XBP-1 by the same order of magnitude, whereas the drug combination doubled the relative amounts of mature XBP-1, consistent with the results for IRE1. None of the two agents induced cleavage of ATF6 individually, whereas the combination increased the active form of ATF6. Thus, bortezomib and ritonavir synergistically trigger the UPR via different major activation routes.

JNK and c-JUN were phosphorylated and expressed in increased amounts in HT1080 cells only after treatment with the drug combination, whereas the individual agents showed no effect. A similar picture was observed when the activation of the caspase-4, caspase-9, and caspase-8 was addressed. Only the drug combination resulted in induction of the active species of caspase-4 and caspase-9. Caspase-8 showed some activation after bortezomib treatment, as expected, but this did not further increase on addition of ritonavir.

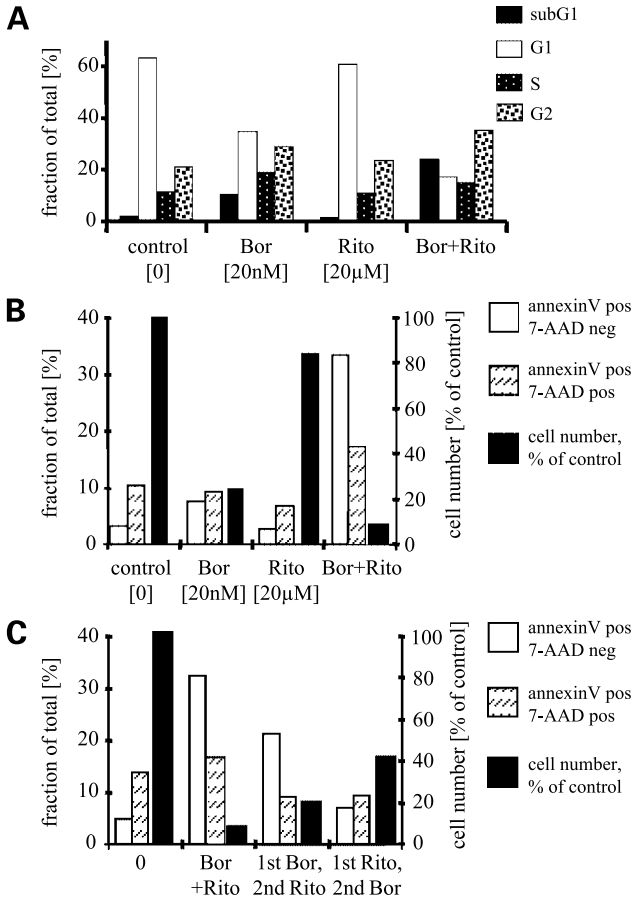

Figure 4. Simultaneous application of ritonavir augments the effect of bortezomib on cell cycling and is more effective than sequential application. **A,** ritonavir does not affect cell cycle at therapeutic drug levels but augments the effect of bortezomib. HT1080 growing in exponential phase were incubated with 20 nmol/L bortezomib, 20 μmol/L ritonavir, or the combination of both for 16 h and DNA contents were assessed by propidium iodine staining. The relative representation of the different phases of cell cycling after the respective treatment is displayed. **B,** therapeutic plasma levels of ritonavir amplify the effect of bortezomib on cell viability. HT1080 cells incubated with ritonavir and/or bortezomib as in **A** were stained with Annexin V [for detecting the fraction of (early) apoptotic cells] and 7-aminoactinomycin D (for detecting late apoptotic or already dead cells) and analyzed by fluorescence-activated cell sorting. *Y axis, left,* relative fraction of early/late apoptotic cells under either treatment (*open columns*); *y axis, right,* decrease in total cell number relative to untreated control cells is (*filled columns*). **C,** simultaneous application of bortezomib and ritonavir is more effective than sequential application of both substances. HT1080 cells were incubated with 20 nmol/L bortezomib for 16 h followed by 20 μmol/L ritonavir for 16 h (and vice versa) or with the combination of both substances (16 h both substances, 16 h culture medium). Total cell numbers are expressed relative to the untreated control (*filled column, y axis, right*) and the proportions of early/late apoptotic cells (Annexin V/7-aminoactinomycin D) are displayed as before (*y axis, left*).

Ritonavir Promotes the Induction of G_2 Arrest by Bortezomib in Sarcoma Cells

We next analyzed whether bortezomib, ritonavir, and/or the combination of both drugs would affect cell cycling in sarcoma cells in a synergistic manner (Fig. 4). Bortezomib treatment increased the proportion of sarcoma cells in S and G_2 phase while proportionally decreasing the fraction of cells in G_1 phase by ~50%, consistent with a G_2 arrest. Ritonavir, by contrast, did not influence cycling. The combination of bortezomib and ritonavir led to a 6-fold increase in cells in sub-G_1 phase, consistent with the induction of apoptosis in the same order of magnitude (Fig. 4B). The sequential exposure of sarcoma cells to both drugs was less effective than their simultaneous addition (Fig. 4C).

Ritonavir Is a Potent Inhibitor of Cellular Protein Turnover in Sarcoma Cells

HIV protease inhibitors have repeatedly been claimed to modulate proteasome function and/or cellular protein turnover. However, the nature of these effects is poorly understood (22–24). We pulse labeled newly synthesized protein in RD cells with [^{35}S]methionine/cysteine for 15 min in the presence/absence of bortezomib (20 nmol/L), ritonavir (20 μmol/L), or the combination of the two agents. Cell cultures were further cultivated at 37°C for 60 min (chase) to allow for spontaneous protein turnover. Identical numbers of cells were lysed, and lysates were treated with ice-cold 10% TCA to precipitate the radioactivity incorporated in proteins and the decrease in the amount of this TCA-sensitive radioactivity quantified over time.

After the pulse, significantly lower amounts of radioactivity were incorporated by bortezomib-treated cells then by control cells, consistent with a UPR induction leading to decreased protein biosynthesis (Fig. 5A). A less pronounced effect was detected with ritonavir-treated cells, consistent with the poorer phosphorylation of eIF2α. Maximum suppression of protein biosynthesis was observed in cells treated with the combination of both drugs.

The highest rate of protein degradation (loss of TCA-sensitive radioactivity/time) was again observed in cells incubated without any drug as expected (arbitrarily defined as 100%; Fig. 5A, *bottom*). Bortezomib treatment

reduced this rate of protein destruction by 66% (range, 61-71%). Strikingly, ritonavir led to a 85% (range, 71-97%) decrease in the breakdown of radiolabeled protein already at the 20 μmol/L concentration. The combination of both drugs reduced the rate of protein destruction by 89% (range, 85-94%). The inhibition of total protein breakdown was significantly stronger when cells were treated with the combination of both drugs compared with bortezomib monotherapy ($P = 0.03$).

When we analyzed the accumulation of polyubiquitinated proteasome substrates (Fig. 5B), we observed a modest accumulation in bortezomib-treated cells but virtually no accumulation in ritonavir-treated cells, although the inhibition of protein degradation was higher in ritonavir-treated cells than after bortezomib treatment. The combination of both drugs strongly induced the accumulation of ubiquitinated proteasome substrates, indicating that it targets the cytosolic ERAD machinery.

Discussion

We provide evidence that pharmacologic induction of ER stress by ritonavir sensitizes sarcoma cells toward apoptosis induction by bortezomib. This may allow to better exploit the therapeutic potential of proteasome inhibition in solid malignancies. We show that (*a*) significant UPR induction can be achieved by ritonavir, a licensed drug, at clinically relevant concentrations; (*b*) such pharmacologically induced UPR can amplify the UPR induced by bortezomib and convert it into a terminal UPR leading to apoptosis; and (*c*) this pharmacologic UPR induction is sufficient to sensitize ''low ER stress''–type, bortezomib-insensitive malignant cells such as sarcoma to bortezomib-induced apoptosis.

The UPR restores cellular integrity, promoting cell survival. However, excess UPR activation leads to a terminal UPR, which directly results in apoptosis, eliminating the defective cell (7). Malignant cells are characterized by increased basal ER stress and UPR activation, possibly due to their higher rate of production of defective protein, compared with nonmalignant cells (25–28). This may allow one to selectively eliminate malignant cells by appropriately increasing the degree of ER stress. However, apart from bortezomib, we currently lack licensed drugs that may be used as UPR-inducing agents, although some UPR-inducing capacity has been shown for cisplatin (29). Indeed, tunicamycin, a laboratory standard for induction of ER stress, sensitizes malignant cells toward bortezomib-induced apoptosis (29). Ritonavir, as we here show, is not only at least similarly efficient in this respect but also less toxic, licensed, and orally available.

Bortezomib blocks the cytosolic degradation of misfolded protein after its retrograde transport form the ER, while at the same time it directly interferes with the compensatory UPR pathway, favoring the terminal UPR (6, 8, 30, 31). ''High ER stress'' types of malignancies, such as myeloma and pancreatic cancer, are characterized by extensive protein secretion (8, 26, 32). They are bortezomib sensitive and can be further sensitized toward bortezomib-mediated apoptosis when additional ER stress is induced (29). By contrast, the sensitivity of nonsecretory malignancies such as sarcoma toward bortezomib is poor, both *in vitro* and

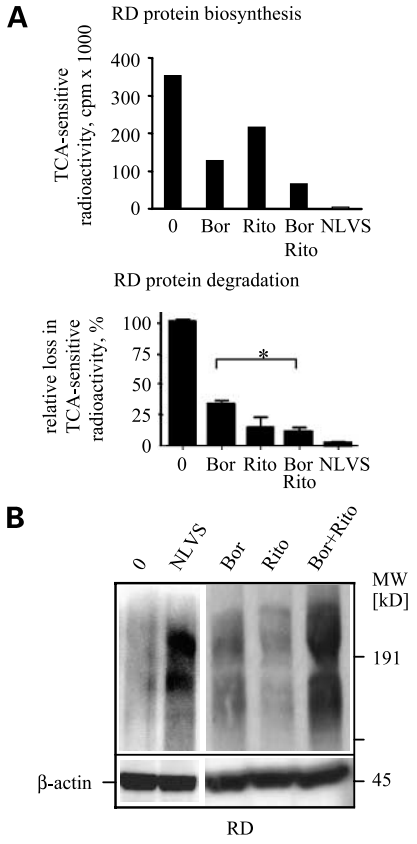

Figure 5. Ritonavir inhibits cellular protein biosynthesis and degradation in sarcoma cells. **A,** effects of ritonavir and bortezomib on total protein biosynthesis and degradation. *Top,* RD cells were incubated with 20 nmol/L bortezomib, 20 μmol/L ritonavir, or the combination of both for 16 h and metabolic labeling of total protein biosynthesis was done with [^{35}S]-methionine/cysteine for 15 min (pulse) as detailed in Materials and Methods. Cells incubated in NLVS (50 μmol/L) served as additional control. To assess total protein biosynthesis, total cellular protein was precipitated with ice-cold TCA from lysates prepared from equal cell numbers. Incorporated radioactivity was measured using a scintillation counter and displayed relative to the untreated control. Representative of three experiments. *Bottom,* to assess the relative rates of protein degradation under either treatment, equal numbers of cells were pulse labeled as before and further cultured in complete medium for 60 min (chase). Cells were lysed, and the incorporated radioactivity was determined as before. The loss in incorporated radioactivity during the chase was determined and calculated relative to the amount of incorporated radioactivity measured after the pulse. In untreated control cells, this ratio was arbitrarily set as 100 and compared with the ratios in the treated samples to mirror the rate of bulk protein degradation under either treatment independent from the absolute amount of incorporated radioactivity. Mean ± SE of three independent experiments. The difference in this loss of radioactivity between cells treated with bortezomib alone and cells treated with bortezomib + ritonavir was statistically significant using Student's *t* test ($P < 0.05$). **B,** combination of ritonavir and bortezomib leads to the accumulation of polyubiquitinated protein. RD cells were treated with 20 nmol/L bortezomib, 20 μmol/L ritonavir, the combination of both, or 50 μmol/L NLVS. The levels of polyubiquitinated protein as well as β-actin were assessed by Western blot from equal amounts of total cellular protein.

clinically, consistent with the relatively low degree of constitutive ER stress in sarcoma cells (''low ER stress'' type of cancer). Artificial induction of a ''high ER stress'' situation could lower the threshold for induction of a terminal UPR also in ''low ER stress'' types of cancers such as sarcoma. This would allow bortezomib to trigger UPR-mediated apoptosis also in these types of cells.

The HIV protease inhibitor ritonavir is cytotoxic for different types of malignant cells *in vitro*, albeit at relatively high concentrations (13), and induces regression of certain types of malignancies *in vivo*. The underlying mechanism for this remains largely unclear (14, 15, 33). Ritonavir treatment can lead to severe dyslipidemia and atherosclerosis *in vivo*, which has been linked to the induction of ER stress and apoptosis in hepatocytes and macrophages (11). Based on our results, ritonavir efficiently induces ER stress in sarcoma cells and can result in apoptosis via induction of a terminal UPR. The direct cytotoxic effect of ritonavir on sarcoma cell lines, however, was only observed at very high concentrations of the drug that are well above the therapeutic range of 5 to 20 μmol/L.

Whereas neither bortezomib nor ritonavir monotherapy induced significant cytotoxicity in sarcoma cells at therapeutic drug levels, the combination resulted in robust apoptosis and induction of >90% cell death. A molecular basis for this synergistic effect was provided by our analysis of the UPR-activating pathways: ritonavir mainly induced activation of the IRE1 pathway, which was not triggered by bortezomib, whereas bortezomib activated the PERK pathway stronger than ritonavir but did not induce IRE1 activation. Only the combination of both drugs and therefore the simultaneous triggering of both activation pathways induced the UPR sufficiently strong to induce the apoptotic cascade. However, apoptosis is likely mediated via additional apoptotic pathways, because inhibition of JNK or caspase-4 did not interfere with apoptosis induction by bortezomib combined with ritonavir (data not shown).

The interaction between HIV protease inhibitors and the proteasome has been analyzed over the past decade, and both inhibitory and activating effects have been described (22–24). The effects of ritonavir on the UPR and ERAD machinery observed here are also not easily to be reconciled to predict a single molecular target for ritonavir: we show that ritonavir does not affect the activity of proteasomal active sites in contrast to bortezomib. However, it very efficiently decreases overall protein degradation without significant accumulation of ubiquitinated protein intermediates and furthermore activates the IRE1 trigger of the UPR. This suggested that ritonavir at therapeutic concentrations could act mainly on the ER level, for example, by causing defective protein biosynthesis or preventing the retrotranslocation of misfolded protein. However, the combination of bortezomib and ritonavir synergistically increased the accumulation of polyubiquitinated protein in comparison with bortezomib alone, so that ritonavir, at least in the presence of bortezomib, is likely to also have a cytosolic target related to the proteasome. Ritonavir might therefore even have more than one molecular target depending on the doses and the presence or absence of bortezomib. Ritonavir has been suggested to bind to a yet unidentified noncatalytic modifier site of proteasome function (34). Recently, the zinc metalloprotease ZMPSTE24 that is involved in the activation of ATF6 has been identified as another target of HIV protease inhibitors (35).

Our data provide the first proof of concept that a combined targeting of the UPR by bortezomib and HIV protease inhibitors can render poorly bortezomib-sensitive, low ER stress types of solid malignancies bortezomib sensitive. Obviously, this concept awaits clinical confirmation. Because ritonavir is a licensed drug for HIV therapy, this transition from bench to bedside may be done relatively quickly. In addition, the exact molecular target of ritonavir remains to be explored as well as to whether other types of HIV protease inhibitors will have a similar effect on UPR induction and the cytotoxic effect of bortezomib (36).

Disclosure of Potential Conflicts of Interest

No potential conflicts of interest were disclosed.

Acknowledgments

We thank H.M. Jäck and R. Voll (Department for Molecular Immunology, University of Erlangen) for a critical review of the article and the very helpful and open discussions.

References

1. Rajkumar SV, Richardson PG, Hideshima T, Anderson KC. Proteasome inhibition as a novel therapeutic target in human cancer. J Clin Oncol 2005;23:630–9.

2. Glickman MH, Ciechanover A. The ubiquitin-proteasome proteolytic pathway: destruction for the sake of construction. Physiol Rev 2002;82:373–428.

3. Altun M, Galardy PJ, Shringarpure R, et al. Effects of PS-341 on the activity and composition of proteasomes in multiple myeloma cells. Cancer Res 2005;65:7896–901.

4. Lightcap ES, McCormack TA, Pien CS, et al. Proteasome inhibition measurements: clinical application. Clin Chem 2000;46:673–83.

5. Ovaa H, van Swieten PF, Kessler BM, et al. Chemistry in living cells: detection of active proteasomes by a two-step labeling strategy. Angew Chem Int Ed Engl 2003;42:3626–9.

6. Gass JN, Gunn KE, Sriburi R, Brewer JW. Stressed-out B cells? Plasma-cell differentiation and the unfolded protein response. Trends Immunol 2004;25:17–24.

7. Zhang K, Kaufman RJ. The unfolded protein response: a stress signaling pathway critical for health and disease. Neurology 2006;66:S102–9.

8. Davenport EL, Moore HE, Dunlop AS, et al. Heat shock protein inhibition is associated with activation of the unfolded protein response (UPR) pathway in myeloma plasma cells. Blood 2007;110:2641–9.

9. Catley L, Weisberg E, Kiziltepe T, et al. Aggresome induction by proteasome inhibitor bortezomib and alpha-tubulin hyperacetylation by tubulin deacetylase (TDAC) inhibitor LBH589 are synergistic in myeloma cells. Blood 2006;108:3441–9.

10. Nawrocki ST, Carew JS, Dunner K Jr, et al. Bortezomib inhibits PKR-like endoplasmic reticulum (ER) kinase and induces apoptosis via ER stress in human pancreatic cancer cells. Cancer Res 2005;65:11510–9.

11. Zhou H, Pandak WM Jr, Lyall V, Natarajan R, Hylemon PB. HIV protease inhibitors activate the unfolded protein response in macrophages: implication for atherosclerosis and cardiovascular disease. Mol Pharmacol 2005;68:690–700.

12. Sgadari C, Monini P, Barillari G, Ensoli B. Use of HIV protease

inhibitors to block Kaposi's sarcoma and tumour growth. Lancet Oncol 2003;4:537 – 47.

13. Gaedicke S, Firat-Geier E, Constantiniu O, et al. Antitumor effect of the human immunodeficiency virus protease inhibitor ritonavir: induction of tumor-cell apoptosis associated with perturbation of proteasomal proteolysis. Cancer Res 2002;62:6901 – 8.

14. Dewan MZ, Uchihara JN, Terashima K, et al. Efficient intervention of growth and infiltration of primary adult T-cell leukemia cells by an HIV protease inhibitor, ritonavir. Blood 2006;107:716 – 24.

15. Pati S, Pelser CB, Dufraine J, et al. Antitumorigenic effects of HIV protease inhibitor ritonavir: inhibition of Kaposi sarcoma. Blood 2002;99: 3771 – 9.

16. Glas R, Bogyo M, McMaster JS, Gaczynska M Ploegh HL. A proteolytic system that compensates for loss of proteasome function. Nature 1998;392:618 – 22.

17. Nicoletti I, Migliorati G, Pagliacci MC, Grignani F, Riccardi C. A rapid and simple method for measuring thymocyte apoptosis by propidium iodide staining and flow cytometry. J Immunol Methods 1991;139:271 – 9.

18. Berkers CR, Verdoes M, Lichtman E, et al. Activity probe for *in vivo* profiling of the specificity of proteasome inhibitor bortezomib. Nat Methods 2005;2:357 – 62.

19. Greiner A, Lautwein A, Overkleeft HS, Weber E, Driessen C. Activity and subcellular distribution of cathepsins in primary human monocytes. J Leukoc Biol 2003;73:235 – 42.

20. Driessen C, Bryant RA, Lennon-Dumenil AM, et al. Cathepsin S controls the trafficking and maturation of MHC class II molecules in dendritic cells. J Cell Biol 1999;147:775 – 90.

21. Kraus M, Ruckrich T, Reich M, et al. Activity patterns of proteasome subunits reflect bortezomib sensitivity of hematologic malignancies and are variable in primary human leukemia cells. Leukemia 2007;21:84 – 92.

22. Andre P, Groettrup M, Klenerman P, et al. An inhibitor of HIV-1 protease modulates proteasome activity, antigen presentation, and T cell responses. Proc Natl Acad Sci U S A 1998;95:13120 – 4.

23. Pajonk F, Himmelsbach J, Riess K, Sommer A, McBride WH. The human immunodeficiency virus (HIV)-1 protease inhibitor saquinavir inhibits proteasome function and causes apoptosis and radiosensitization in non-HIV-associated human cancer cells. Cancer Res 2002;62: 5230 – 5.

24. Schmidtke G, Holzhutter HG, Bogyo M, et al. How an inhibitor of the HIV-I protease modulates proteasome activity. J Biol Chem 1999;274: 35734 – 40.

25. Scriven P, Brown NJ, Pockley AG, Wyld L. The unfolded protein response and cancer: a brighter future unfolding? J Mol Med 2007;85: 331 – 41.

26. Obeng EA, Carlson LM, Gutman DM, et al. Proteasome inhibitors induce a terminal unfolded protein response in multiple myeloma cells. Blood 2006;107:4907 – 16.

27. Feldman DE, Chauhan V, Koong AC. The unfolded protein response: a novel component of the hypoxic stress response in tumors. Mol Cancer Res 2005;3:597 – 605.

28. Koumenis C, Wouters BG. ''Translating'' tumor hypoxia: unfolded protein response (UPR)-dependent and UPR-independent pathways. Mol Cancer Res 2006;4:423 – 36.

29. Nawrocki ST, Carew JS, Pino MS, et al. Bortezomib sensitizes pancreatic cancer cells to endoplasmic reticulum stress-mediated apoptosis. Cancer Res 2005;65:11658 – 66.

30. Iwakoshi NN, Lee AH Glimcher LH. The X-box binding protein-1 transcription factor is required for plasma cell differentiation and the unfolded protein response. Immunol Rev 2003;194:29 – 38.

31. Iwakoshi NN, Lee AH, Vallabhajosyula P, et al. Plasma cell differentiation and the unfolded protein response intersect at the transcription factor XBP-1. Nat Immunol 2003;4:321 – 9.

32. Meister S, Schubert U, Neubert K, et al. Extensive immunoglobulin production sensitizes myeloma cells for proteasome inhibition. Cancer Res 2007;67:1783 – 92.

33. Ikezoe T, Hisatake Y, Takeuchi T, et al. HIV-1 protease inhibitor, ritonavir: a potent inhibitor of CYP3A4, enhanced the anticancer effects of docetaxel in androgen-independent prostate cancer cells *in vitro* and *in vivo*. Cancer Res 2004;64:7426 – 31.

34. Schmidtke G, Emch S, Groettrup M, Holzhutter HG. Evidence for the existence of a non-catalytic modifier site of peptide hydrolysis by the 20S proteasome. J Biol Chem 2000;275:22056 – 63.

35. Coffinier C, Hudon SE, Farber EA, et al. HIV protease inhibitors block the zinc metalloproteinase ZMPSTE24 and lead to an accumulation of prelamin A in cells. Proc Natl Acad Sci U S A 2007;104:13432 – 7.

36. Gills JJ, Lopiccolo J, Tsurutani J, et al. Nelfinavir, A lead HIV protease inhibitor, is a broad-spectrum, anticancer agent that induces endoplasmic reticulum stress, autophagy, and apoptosis *in vitro* and *in vivo*. Clin Cancer Res 2007;13:5183 – 94.